Improved accuracy in 2D/3D registration for image guided radiotherapy by using kV-MV image pairs

Hugo Furtado[13], Michael Figl[13], Markus Stock[23], Dietmar Georg[23], and Wolfgang Birkfellner[13]

[1] Center for Biomedical Engineering and Physics, Medical University Vienna, Austria
[2] Department of Radiation Oncology, Medical University Vienna, Austria
[3] Christian Doppler Laboratory for Medical Radiation Research for Radiation Oncology, Medical University Vienna, Austria

Abstract. Patient motion during radiotherapy (intra-fractional motion), is one of the major sources of uncertainty in dose application. 2D/3D registration is an intensity based method used successfully to track tumor motion with the potential to reduce uncertainty. Despite promising results, the direction perpendicular to the 2D imaging plane cannot be accurately resolved leading to an incomplete, five-degrees-of freedom tracking. In this paper, we propose the use of two 2D images to improve registration results. Modern LINACs have the ability to acquire mega-voltage images, with significantly different contrast, simultaneously to the kilo-voltage image acquisition. Our results show that, when using both images, registration accuracy in all six degrees of freedom dramatically improves. This means that accurate motion tracking can be performed and it integrates easily with the clinical workflow.

Keywords: 2D/3D registration, motion tracking, radiation therapy, kilo-Voltage/mega-Voltage

1 Introduction

One of the major sources of uncertainty in dose application during radiotherapy is patient motion during the treatment or intra-fractional motion. Periodic motion related to the breathing cycle or heartbeat and other forms of aperiodic motion require the enlargement of the planned target volume (PTV) to make sure the full tumor is correctly irradiated. The most important consequence is that dose delivery is increased to healthy tissue.

Tumor motion tracking can help reduce the PTV by reducing the uncertainty about tumor position and help deliver more precise therapy. In the case of lung tumors, approaches to motion tracking include tracking of implanted fiducial markers [10], magnetic transponders [11], external surrogate markers [2] and correlation of external motion with lung motion models [9]. Recently, the CyberKnife® system has also the possibility of intensity based markerless tumor tracking using two cameras [1] where the the tumor position is detected at

certain points of the breathing cycle and correlated to external markers. Purely intensity based 2D/3D registration [4] is an important approach as it does not require markers or fiducials to be implanted and can deal well with aperiodic motion. Despite promising results, an intrinsic problem with this approach is the inability to accurately resolve displacement occurring in the direction perpendicular to the imaging plane [12].

Modern LINACs have not only the ability to acquire portal kiloVoltage (kV) images during treatment but also the possibility to acquire a megaVoltage (MV) image using the treatment beam. The two images are, at least in the case of the Elekta^{TM} treatment machines, perpendicular and they can both be used for 2D/3D registration. In this paper, we present a comparison of registration results when using only one kV image or when using different combinations of kV and MV images. We evaluated the different combinations using a porcine phantom data set and standard patient data. Our results on both data sets show that when using both images registration accuracy increases, leading to more accurate motion tracking in six degrees-of-freedom.

2 Materials and methods

2.1 2D/3D registration

2D/3D registration is a widely used approach in image guided interventions [6]. In a first step, a simulated x-ray image - a DRR - is generated from a 3D volume by a ray casting algorithm, simulating the attenuation of virtual x-rays. The DRR image is then compared to the x-ray image acquired during treatment by means of a merit function. An optimizer searches for the spatial transformation which generates the best match between the DRR and the x-ray. The final translational and rotational parameters $(t_x, t_y, t_z, \omega_x, \omega_y, \omega_z)$ represent the tumor displacement. In this work we used a mutual information (MI) [3] based merit function and the optimization was performed using the Powel optimizer [8].

2.2 Image datasets and Image preprocessing

For the evaluation, we used a freely available porcine head dataset [7] and images from a patient undergoing routine treatment in our clinic. From the porcine dataset we used computed tomography (CT) 3D images and four 2D images: two kV images taken from lateral (LAT) and anterior-posterior (AP) views and two MV images taken from the same views. The gold-standard transformation between all images is available. Because the porcine head features soft tissue which can deform, registration was performed on a region of interest (ROI). Figure 1 shows the 2D images for the LAT view and the ROI mask used.

The patient dataset consists of images from a patient suffering from non-small cell lung cancer undergoing regular treatment in our clinic. We used a planning CT volume where the tumor margins and organs at risk were delineated in a standard planning procedure, a sequence of (151) kV x-ray images and a sequence

of (52) MV x-ray images acquired simultaneously during treatment with rates of approximately 5.4 Hz and 2 Hz respectively. The registration is done on a region of interest (ROI) centered around the PTV for two reasons: (a) the PTV is the region where we want to follow motion and where the assumption of a rigid transformation is valid and (b) rendering a smaller area is also less time consuming as there are less pixels to render. Figure 2 shows a CT slice with the planning contoured structures (left) and one kV x-ray and one MV x-ray with the structures projected on them (center and right).

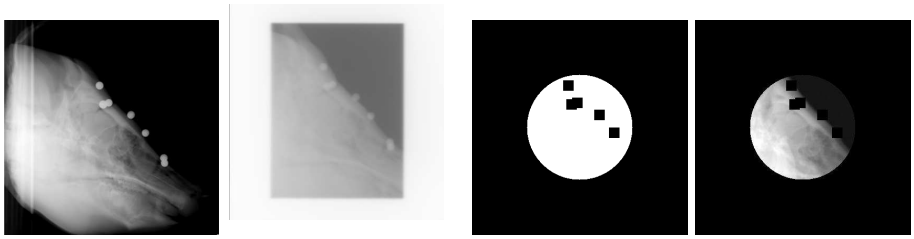

Fig. 1. Pig 2D image data: The first column shows a kV images from lateral view, the second column a correponding MV image, the third, the mask used for the ROI and the last column shows the kV image after masking

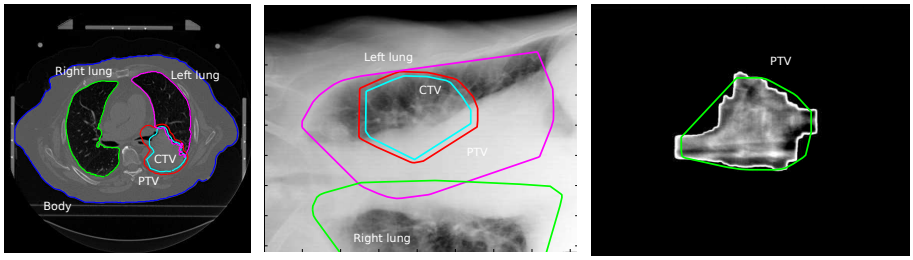

Fig. 2. Patient image data: On the left a slice of the planning CT with the planning structures is shown, on the center the structure were projected on an X-ray acquired during treatment and on the right, only the PTV was projected on an EPID image acqured during treatment.

The sequence of patient kV and MV images, was acquired with different rates. The sample rate ratio was not accurately known and so, the time correspondence between images was not defined. To find this correspondence, first the ground truth motion was extracted from both sequences by segmenting visible features on the images (e.g. the diaphragm). Then, the motion with lower sample rate (MV) was iteratively re-sampled until a maximum of cross correlation between both motion signals was found.

2.3 Evaluation methodology

We followed slightly different evaluation approaches for each of the datasets as they have different characteristics. In the case of the pig, only static images are available but with a well known gold standard. In the case of the patients, there is no gold standard but a fluoroscopic image sequence was available. The general approach consisted in comparing the accuracy of the 2D/3D registration using only one 2D image and 2D image pairs.

For the pig dataset, the accuracy evaluation was performed following the methodology proposed by [5] where a mean target registration error (mTRE) metric is used. The mTRE, consists of the mean of distances between target points spread evenly on the volumes, transformed by the ground truth, and by the transformation obtained with the registration method. We compared registrations performed using only one 2D image (referred to as 1-kV), one kV and one MV image (kV-MV) and two kV images (2-kV). For each of the combinations we evaluated the registration results using 250 initial displacements, chosen randomly, which are offsets of the gold standard. The total initial mTRE ranges from 0 to 25 mm in steps of 1 mm with 10 points at each step.

For the patients, we performed different registration sequences attempting to extract tumor motion as described in [4]. To compare performance, we extracted motion in 5 degrees-of-freedom (DOF) using only the kV sequence, in 6 DOF using only the MV sequence and in 6 DOF using a sequence of kV-MV image pairs. In the latter case, we used a subset (52) of the kV images that approximately corresponds to the MV image sequence in time.

Although there is no gold standard available, we also performed an evaluation similar to the pig dataset, where we used a pair of 2D images (kV-MV) that correspond well in time, and evaluated results using 150 initial displacements from an initial point, evaluating the coherence of registration results. The total initial mTRE ranges from 0 to 15 mm in steps of 1 mm.

3 Results

The results obtained for the pig dataset are shown in table 1 as mean and standard deviation final mTRE for all the registrations. Figure 3 shows a plot of individual registration results leaving out results that are above 25 mm. Table 2 shows the mean, standard deviation and rms of the error of the final translation parameters in relation to the gold standard summarizing the error data for all registrations.

Regarding the patient resuls, figure 4 shows the reconstructed tumor centroid motion along the cranial-caudal (CC, blue line), left-right (LR green line) and anterion-posterior (AP red line) directions in 5 DOF using only the kV image sequence for registration. The black dashed line shows the extracted diaphragm motion. The major contribution to the motion is in the CC direction as was seen in our previous work [4]. Figure 5 shows a plot of the extracted tumor centroid motion along the AP direction (the direction perpendicular to the kV

	mTRE: MEAN ± STD (mm)
1-kV	4.9 ± 4.1
kV-MV	1.8 ± 1.1
2-kV	1.7 ± 1.3

Table 1. Mean (MEAN) and standard deviation (STD) of mTREs for the different image combinations.

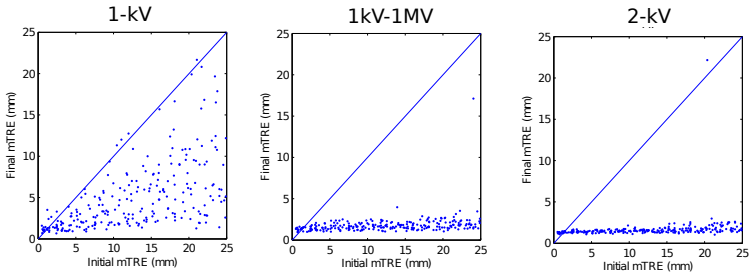

Fig. 3. Plots of individual registration results for each of the image combinations: one kV image (first row), one kV and one MV images (second row) and two kV images calculated using a mutual information based merit function.

	error t_x (mm)		error t_y (mm)		error t_z (mm)	
2D image	MEAN ± STD	RMS	MEAN ± STD	RMS	MEAN ± STD	RMS
1-kV	0.2 ± 0.2	0.3	-0.3 ± 0.3	0.4	0.1 ± 5.7	5.7
1kV-1MV	0.3 ± 0.1	0.3	-0.2 ± 0.1	0.3	-1.0 ± 0.5	1.1
2-kV	0.4 ± 0.1	0.5	-0.5 ± 0.1	0.5	-0.2 ± 0.2	0.3

Table 2. Summary of the offset error in relation to the gold standard for the three translation parameters, X, Y and Z. The offset errors are shown as the mean (MEAN) ± standard deviation (STD) and the root mean square (RMS) error.

imaging plane) for three registration combinations: 5 DOF with one 2D image sequence, 6 DOF with one 2D image sequence and 6 DOF with a kV-MV image pair sequence. The motion along the AP direction ranges from very little to up to 25 mm in the case of registration in 6 DOF with only one 2D image sequence. Table 3 summarizes these results as a mean, standard deviation and RMS amplitute of the motion in the AP direction for the three registration sequences.

Finally, figure 6 shows a comparison of the final registration translation parameter t_z (shown as offset to the mean), for 150 starting positions with increasing initial mTRE when using only one kV image (left) and a kV-MV image pair (right). Table 4 summarizes these results as mean and standard deviation of the final translation parameters for both cases.

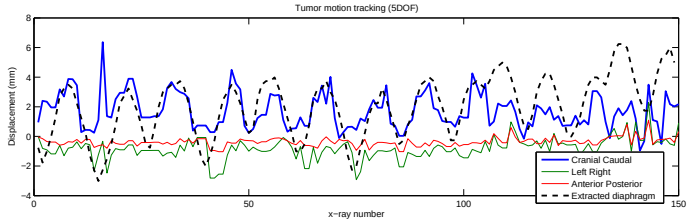

Fig. 4. Reconstructed motion of the centroid of the tumor along CC (blue line), LR (green line), AP (red line) directions for the patient dataset in 5 degrees of freedom using only the kV image sequence. The diaphragm motion is also shown as a black dotted line. Note that some outliers are omitted in the case of the AP direction.

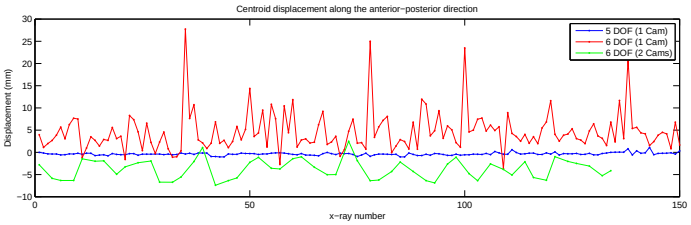

Fig. 5. Reconstructed motion of the centroid of the tumor along the AP direction for the patient dataset, in 5 DOF using one 2D image for registration (blue line) in 6 DOF using one 2D image for registration and in 6 DOF using two 2D images for registration.

4 Discussion and Conclusions

Our results demonstrate the improvement on accuracy by using two 2D images in the 2D/3D registration. For the pig dataset, it is easily seen in figure 3 that when only one image is used, the mTRE increases as the initial displacement also increases. The large errors stem from a random final t_z parameter as this translation cannot be accurately resolved with only one projection. The data in table 1 and table 2 confirm this finding showing that the final mTRE and

	Motion along AP direction (mm)	
2D image	MEAN ± STD	RMS
1-kV (5DOF)	-0.37 ± 0.3	0.48
1-kV (6DOF)	4.61 ± 4.52	6.45
2-kV (6DOF)	-3.78 ± 2.22	4.37

Table 3. Summary of the tumor centroid motion along the AP direction shown as the mean (MEAN) ± standard deviation (STD) and RMS of the amplitude of the set of registrations over time.

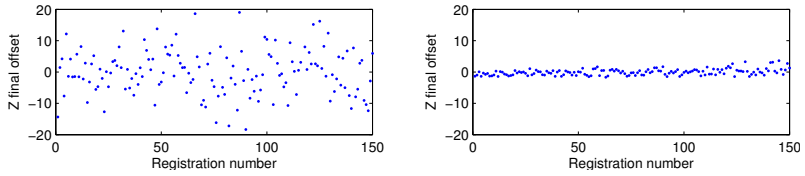

Fig. 6. Plots of the offset to the mean of the final translation parameter t_z for the individual registrations on the patient data shown for the two a image combinations, 1-kV and 1kV-1MV

	t_x (mm)	t_y (mm)	t_z (mm)
2D image	MEAN ± STD	MEAN ± STD	MEAN ± STD
1-kV	4.94 ± 1.89	-7.55 ± 2	545.83 ± 7.4
1kV-1MV	13.38 ± 1.14	-3.84 ± 1.63	534.78 ± 1.07

Table 4. Summary of the offset error in relation to the gold standard for the three translation parameters, X, Y and Z. The offset errors are shown as the mean (MEAN) ± standard deviation (STD) and the root mean square (RMS) error of the offset of the gold standard. The registration was calculated for the four different merit functions.

the parameter error is much lower when an image pair is used. The results are slightly better when two kV images are used but typically, there is only the possibility of acquiring a kV-MV image pair during treatment.

For the patient dataset, tumor motion could be tracked in 5 DOF with reasonable accuracy. Figure 4 shows good correlation between extracted diaphragm motion and tumor motion obtained by registration. It is evident from figure 5 that extracting tumor motion in 6 DOF using only a kV image sequence for registration leads to high inaccuracy. It is known that there is almost no motion in the AP direction so we can conclude that the extracted motion is incorrectly resolved, as large displacements (red line) are shown. When using a sequence of image pairs (green line) the motion is again much smaller. Table 3 also shows that both the standard deviation and the RMS of the motion amplitude are significantly smaller when an image pair sequence is used.

Finally, in figure 6 the displacement perpendicular to the imaging plane (here Z direction) is not accurately resolved (left) in contrast with the case when using image pairs (right) where much smaller offset to the mean is obtained. This is also seen in table 4 where a dramatic decrease in standard deviation on the Z translation parameter is shown when using two images for registration.

It is important to say that for the time being, these results are preliminary as accuracy can improve. One of the main sources of uncertainty comes from the fact that the kV and MV image pair sequences do not have a one to one correspondence in the time domain. Further work has to be done to deal with images pairs that are not taken at the same point in time or a synchronization mechanism has to be implemented.

Despite this, taking the presented results into account, we can say that using a pair of images for registration is a good approach to improve accuracy. This is also workflow efficient as acquiring extra MV imaging during treatment adds no additional dose to the patient or burden to the physician.

Acknowledgments. The financial support by the Federal Ministry of Economy, Family and Youth and the National Foundation for Research, Technology and Development is gratefully acknowledged.

References

1. Bibault, J.E., Prevost, B., Dansin, E., Mirabel, X., Lacornerie, T., Lartigau, E.: Image-guided robotic stereotactic radiation therapy with fiducial-free tumor tracking for lung cancer. Radiation Oncology p. 102 (2012), article in press.
2. Cho, B., Poulsen, P.R., Sawant, A., Ruan, D., Keall, P.J.: Real-time target position estimation using stereoscopic kilovoltage/megavoltage imaging and external respiratory monitoring for dynamic multileaf collimator tracking. Int. J. Radiat. Oncol. Biol. Phys. 79(1), 269–78 (2010)
3. Clippe, S., Sarrut, D., Malet, C., Miguet, S., Ginestet, C., Carrie, C.: Patient setup error measurement using 3D intensity-based image registration techniques. International Journal of Radiation Oncology Biology Physics 56(1), 259–265 (2003)
4. Gendrin, C., Furtado, H., Weber, C., Bloch, C., Figl, M., Pawiro, S., Bergmann, H., Stock, M., Fichtinger, G., Georg, D., Birkfellner, W.: Monitoring tumor motion by real time 2d/3d registration during radiotherapy. Radiotherapy and Oncology 102(2), 274–280 (2012)
5. van de Kraats, E.B., Penney, G.P., Tomaževič, D., van Walsum, T., Niessen, W.J.: Standardized evaluation methodology for 2-D-3-D registration. IEEE Transactions on Medical Imaging 24(9), 1177–1189 (2005)
6. Markelj, P., Tomaževič, D., Likar, B., Pernuš, F.: A review of 3d/2d registration methods for image-guided interventions. Med. Image Anal. In press (2010)
7. Pawiro, S.A., Markelj, P., Pernuš, F., Gendrin, C., Figl, M., Weber, C., Kainberger, F., Noebauer-Huhmann, I., Bergmeister, H., Stock, M., Georg, D., Bergmann, H., Birkfellner, W.: Validation for 2d/3d registration. i: A new gold standard data set. Med. Phys. 38(3), 1481–1490 (2011)
8. Powell, M.: Nonconvex Optimization and Its Applications, chap. The NEWUOA sorftware for unconstrained optimization without derivatives, pp. 255–297. Springer US (2006)
9. Ren, Q., Nishioka, S., Shirato, H., Berbeco, R.I.: Adaptive prediction of respiratory motion for motion compensation radiotherapy. Phys. Med. Biol. 52(22), 6651–6661 (2007)
10. Schweikard, A., Glosser, G., Bodduluri, M., Murphy, M.J., Adler, J.R.: Robotic motion compensation for respiratory movement during radiosurgery. Comput. Aided Surg. 5(4), 263–277 (2000)
11. Shah, A.P., Kupelian, P.A., Willoughby, T.R., Langen, K.M., Meeks, S.L.: An evaluation of intrafraction motion of the prostate in the prone and supine positions using electromagnetic tracking. Radiotherapy and Oncology 99(1), 37–43 (2011)
12. Suh, Y., Dietrich, S., Keall, P.J.: Geometric uncertainty of 2d projection imaging in monitoring 3d tumor motion. Phys. Med. Biol. 52, 3439–3454 (2007)